

**Contract No.:**

This manuscript has been authored by Savannah River Nuclear Solutions (SRNS), LLC under Contract No. DE-AC09-08SR22470 with the U.S. Department of Energy (DOE) Office of Environmental Management (EM).

**Disclaimer:**

The United States Government retains and the publisher, by accepting this article for publication, acknowledges that the United States Government retains a non-exclusive, paid-up, irrevocable, worldwide license to publish or reproduce the published form of this work, or allow others to do so, for United States Government purposes.

1 **Nd and Sm Isotopic Composition of Spent Nuclear Fuels from Three**  
2 **Material Test Reactors**

3  
4 Nicholas Sharp<sup>a\*</sup>, Brian W. Ticknor<sup>b</sup>, Michael Bronikowski<sup>b</sup>, Theodore Nichols<sup>b</sup>, William F.  
5 McDonough<sup>c,a</sup>, Alice Mignerey<sup>a</sup>, Donna Beals<sup>b</sup>

6  
7 <sup>a</sup>Department of Chemistry & Biochemistry  
8 University of Maryland  
9 College Park, MD 20742  
10 USA  
11 nicholas.sharp@nist.gov  
12 mignerey@umd.edu

13  
14 <sup>b</sup>Savannah River National Laboratory  
15 Aiken, SC 29808  
16 USA  
17 ticknorbw@ornl.gov  
18 michael.bronikowski@srnl.doe.gov  
19 theodore.nichols@srnl.doe.gov  
20 donnabeals@msn.com

21  
22 <sup>c</sup>Department of Geology  
23 University of Maryland  
24 College Park, MD 20742  
25 USA  
26 mcdonoug@umd.edu

27  
28 \*Corresponding author:  
29 Nicholas Sharp  
30 Materials Measurement Laboratory  
31 National Institute of Standards and Technology  
32 Gaithersburg, MD 20899  
33 USA  
34 Tel: (301) 975-3926  
35 nicholas.sharp@nist.gov

36  
37 Keywords: MC-ICP-MS \* Spent nuclear fuel \* Chromatography \* Nd and Sm isotopic ratios \* Nuclear  
38 forensics

## 39 **Abstract**

40 Rare earth elements such as neodymium and samarium are ideal for probing the neutron  
41 environment that spent nuclear fuels are exposed to in nuclear reactors. The large number of  
42 stable isotopes, some having very large neutron capture cross sections, can provide distinct  
43 isotopic signatures for differentiating the source material for nuclear forensic investigations.  
44 Measurements of the isotopic abundances were carried out by first chromatographically  
45 separating the elements of interest prior to isotopic analysis using multi-collector, inductively  
46 coupled plasma, mass spectrometry (MC-ICP-MS). The rare-earth elements were isolated from  
47 the high activity fuel matrix via ion exchange chromatography in a shielded cell. The resulting  
48 samples then have a low enough activity to be handled outside the glove box or isolated  
49 environment, and the individual elements can be separated using cation exchange  
50 chromatography with alpha-hydroxyisobutyric acid. The neodymium and samarium aliquots  
51 were analyzed via MC-IPC-MS, resulting in isotopic compositions with a precision of 0.01-  
52 0.3 %.

53

## 54 **Introduction**

55 Two types of high-profile nuclear materials in the field of nuclear forensics are pre-  
56 detonation and post-detonation nuclear material. Pre-detonation materials can vary in  
57 composition and complexity from uranium ores to spent nuclear material. Spent nuclear material  
58 represents a unique security concern as it can be used directly in a radiological dispersion device  
59 and it still contains significant amounts of unreacted  $^{235}\text{U}$ . Nuclear fuel from material test  
60 reactors (MTR), a subclass of research reactors, operated with highly enriched  $^{235}\text{U}$  (HEU) fuels,  
61 in some cases up to 93%, until the 1970s when in response to growing security concerns the

62 research reactors were converted to low-enriched fuel (LEU) with enrichments on the order of  
63 20% (1). With their large amount of fissile material and radioactivity, spent nuclear fuels  
64 represent high-profile targets for illicit activities. Methods capable of determining an interdicted  
65 fuel rod's provenance and host-reactor's operating characteristics are required should spent  
66 nuclear fuel provenance ever be questioned (2).

67         During neutron induced fission of  $^{235}\text{U}$  and  $^{239}\text{Pu}$  various rare earth elements (e.g., La-  
68 Dy) are produced on the high-mass tail of the fission curve. Of these elements, Nd, Sm, and Gd  
69 have multiple stable isotopes and are produced in measureable quantities in non-natural isotopic  
70 abundances (3). These elements also have isotopes that have large ( $> 1,000$  b) thermal neutron  
71 capture cross sections, resulting in one-mass heavier isotopes that have negligible ( $\leq 1$  b) capture  
72 cross sections. Consequently, depletion occurs in the large capture cross section isotopes and  
73 enrichment occurs in the low capture cross section isotopes that are proportional to the total  
74 neutron fluence the isotopes have been experienced. Therefore, the absolute and relative isotopic  
75 abundances of Nd, Sm, and Gd can provide important information regarding the type of fissile  
76 material powering a chain reaction along with details about the neutron environment inside the  
77 reactor.

78         In prior studies Nd, Sm, and Gd isotopic composition in spent nuclear fuel have been  
79 analyzed using high-performance liquid chromatography (HPLC) and ion exchange systems  
80 coupled to multi-collector inductively coupled mass spectrometers (MC-ICP-MS) (4-6) to  
81 separate the individual elements. However, both methods require dedicated instrumentation at  
82 least partially contained in a glovebox to perform the separations, which can be logistically  
83 challenging. Other studies (7, 8) have used column chromatography to analyze spent nuclear  
84 fuel from pressurized water reactors, which use fuels that are typically enriched to  $\sim 2\text{-}5\%$   $^{235}\text{U}$ .

85 This study presents a simplified method for separating Nd and Sm from spent nuclear fuel using  
86 a series of cation exchange chromatographic separations optimized for high-dose remote  
87 handling situations allowing subsequent chemistry and analyses to be performed outside of high-  
88 dose environments. The short-lived radionuclides were removed using chromatographic  
89 columns in a shielded cell (9) prior to sample removal. Chromatographic purification of Nd and  
90 Sm were conducted in a radiological hood before being analyzed using multi-collector  
91 inductively coupled plasma mass spectrometry. Spent fuels and reference materials (BHVO-2G,  
92 a powdered basalt) were treated with the same column chemistry, which enabled the reference  
93 materials to serve as a control for mass fractionation correction. The Nd and Sm isotopic  
94 compositions of three spent fuels are compared to determine if specific reactor characteristics  
95 can be distinguished.

## 96 **Materials and Methods**

### 97 Fuel Rod Sampling and Lanthanoid Separation

98 Three MTR spent nuclear fuel assemblies were sampled individually in 2009, 2010, and  
99 2011 (here on referred to as A, B, and C, respectively) at the Savannah River National  
100 Laboratory (SRNL) Shielded Cells Facility. Declared initial and spent  $^{235}\text{U}$  enrichments for each  
101 assembly are listed in Table 1. During each sampling event, the individual fuel assembly was  
102 placed into a containment device inside a shielded cell. The containment device ensured that no  
103 cross contamination occurred between the shielded cells environments and the fuel assemblies.  
104 The spent fuel assemblies from the MTR consisted of multiple plates of uranium fuel spatially  
105 separated from one another and encased in aluminum cladding. Five to six core samples were  
106 excised evenly down the length of the fuel rod, with only the top fuel plate being sampled. The  
107 sampling process provided sufficient mass of material to obtain representative compositional

108 analyses along the length of the fuel rod while minimizing the radioactivity of the processed  
109 solution. The extracted material had an average weight of approximately 1.5 g total with around  
110 0.2 g consisting of the uranium fuel and the rest consisting of the Al-cladding material.

111 The sampled fuels were each dissolved in 100 mL of 50% (v/v) aqua regia. Procedural  
112 blanks were prepared in the containment device for each fuel rod sampling event, resulting in  
113 three blanks labeled Blank A, Blank B, and Blank C with letters identifying the containment  
114 device from which the fuel rod was sampled. These blank solutions were treated identically to  
115 the fuel samples and their concentrations and isotopic abundances are reported along with that of  
116 the fuel rods.

117 All acids (alpha-hydroxyisobutyric, HCl and HNO<sub>3</sub>) used in this work were either  
118 purchased (99.99% grade Optima, Fisher Scientific, Pittsburgh, PA, U.S.A.) or purified using a  
119 triple-distillation process in-house at the University of Maryland (UMD), along with 18 MΩ  
120 water, which was used for dilutions and chemistry. Prior to use, the chromatographic resins  
121 (AG-50W, x8, 200-400 mesh) were cleaned with 6 M HCl and 18 MΩ water rinses. All sample  
122 fractions were collected in acid-leached PTFE containers and standard reference material  
123 chemistry was performed in a class-100 clean laboratory in the Department of Geology at UMD.

124 The lanthanoids were isolated and individually separated similarly to methods developed  
125 for the analysis of trinitite and samples from Oklo (10, 11). Lanthanoid separations for samples  
126 and blanks A-C were performed in the Shielded Cells Facility at SRNL without the use of a  
127 containment device. An aliquot of the 100 mL fuel and blank solutions was transferred to a  
128 scintillation vial pre-marked at the 4 mL volume level. These vials were dried down overnight in  
129 an oven at 70°C and then diluted with 2 mL of 2.0 M HCl. The lanthanoids were separated from  
130 the highly-radioactive fission products (primarily <sup>137</sup>Cs and <sup>90</sup>Sr and their daughters due to

131 significant time between reactor discharge and analysis), uranium, plutonium, and the aluminum-  
132 rich matrix using cleaned cation resin contained in 10 cm x 1.5 cm plastic columns  
133 (Environmental Express R1020) and pre-conditioned with 2.0 M HCl. After loading the samples  
134 onto the columns, the resin was washed with 60 mL of 2.0 M HCl followed by 15 mL of H<sub>2</sub>O  
135 and 50 mL of 2.0 M HNO<sub>3</sub>. The lanthanoids were eluted and collected with 50 mL of 4.0 M  
136 HNO<sub>3</sub>. The resulting solution enriched in lanthanoids was removed from the Shielded Cells  
137 Facility and analyzed using gamma-ray spectroscopy to verify removal of high-activity fission  
138 products.

139 Aliquots of each 50 mL solution (1 mL each, except for sample A where only 0.1 mL  
140 was taken due to the higher total activity of the lanthanoids) were shipped to UMD for separation  
141 of the individual lanthanoids. This separation, which was carried out in a vented laminar flow  
142 hood, certified for radioactive materials, involved the use of AG-50W x8 200-400 mesh resin in  
143 the NH<sub>4</sub><sup>+</sup> form loaded into a 0.3 cm x 28 cm quartz glass column and alpha-hydroxyisobutyric  
144 acid ( $\alpha$ -HIBA) in three strengths 0.15 M, 0.225 M, and 0.53 M all buffered to pH 4.7 using  
145 NH<sub>4</sub>OH (10, 11, 12).

146 The aliquots were dried and reconstituted in 0.2 mL of 0.15 M  $\alpha$ -HIBA and loaded onto  
147 the columns. Following an 8 mL wash of 0.15 M  $\alpha$ -HIBA, the Gd cut was collected in 4.25 mL  
148 of 0.15 M  $\alpha$ -HIBA. A subsequent 8 mL wash of 0.15 M  $\alpha$ -HIBA removed most of the Eu, with  
149 the lighter lanthanoids later collected in 10 mL of 0.53 M  $\alpha$ -HIBA. The column was then  
150 sequentially treated with 6 M HCl, 18 MΩ H<sub>2</sub>O, 7 M NH<sub>4</sub>OH, and equilibrated with 0.225 M  $\alpha$ -  
151 HIBA. The 10 mL aliquot containing the lighter lanthanoids was dried down and the  $\alpha$ -HIBA  
152 digested using aqua regia. The remaining material was reconstituted in 0.2 mL 0.225 M of  $\alpha$ -  
153 HIBA and loaded onto the re-equilibrated column. The column was washed with 3 mL of 0.225

154 M of  $\alpha$ -HIBA. Sm was recovered with 3.75 mL of 0.225 M of  $\alpha$ -HIBA. The column was washed  
155 with 9 mL of 0.225 M of  $\alpha$ -HIBA. Finally, Nd was collected with 4.5 mL of 0.225 M of  $\alpha$ -  
156 HIBA. The Gd, Sm, and Nd aliquots were dried down and the  $\alpha$ -HIBA digested using aqua  
157 regia. These final solutions were then dried down and reconstituted in 2 mL 0.8 M HNO<sub>3</sub> for Sm  
158 and Nd, while Gd was reconstituted in 1 mL 0.8 M HNO<sub>3</sub>. Aliquots of the resulting solutions of  
159 Nd and Sm were taken for MC-ICP-MS analyses while the entire 1 mL Gd solution was  
160 analyzed.

161 Reference materials for this work consisted of BHVO-2 (a basalt powder reference  
162 material from the USGS), a 600 ppb (g/g) solution of lanthanoids (Ce through Dy) in 2 M HCl,  
163 created via dilutions of concentrated elemental stock solutions from Alfa Aesar (referred to as  
164 UMD1), as well as a total procedure blank. Two 0.05 g samples of BHVO-2 were digested using  
165 a mixture of HNO<sub>3</sub> and HF with 100  $\mu$ L of HClO<sub>4</sub> in a sealed 15 mL PTFE beaker at 180°C.  
166 The solution was then dried down and the samples were reconstituted in 6 M HCl, sealed, and  
167 heated for 24 hours. This process was repeated twice and the final dry material was dissolved in  
168 2 mL of 2 M HCl. The reference samples were processed through all chromatographic  
169 separations identically to the fuel rod solutions. In addition a blank (UMD Blank) was prepared  
170 and treated identically to the reference samples. All separations for the reference materials and  
171 UMD Blank were performed in the clean laboratory at UMD and a schematic of the separation  
172 process is shown in Figure 1.

### 173 MC-ICP-MS

174 Isotopic analyses of Nd and Sm were conducted at the Department of Geology, UMD  
175 using a Nu Plasma MC-ICP-MS with operating parameters reported in Table 2. The instrument



176 was coupled to an Aridus I desolvating nebulizer with an uptake rate of 50  $\mu\text{L}/\text{min}$ . The sample  
177 measurement conditions for Nd consisted of 5 blocks of 20 5-second integrations preceded and  
178 followed by a 15-second integration of the background at half a mass unit above the peak. Those  
179 for Sm included 4 blocks of 20 7-second integrations (1 second for Cycle 2) and 15-second  
180 integration for backgrounds. Gd is not reported due to the measured signal being below the  
181 quantification threshold for the fuel samples. Reasons for this will be discussed later.

182 Instrument induced mass fractionation was corrected with the standard-sample-standard  
183 bracketing method using the UMD1 solution as the standard and the BHVO-2 samples as a  
184 quality control check to determine the accuracy of the correction method. In addition the AMES  
185 Nd isotopic standard was diluted to give similar signal intensity as the samples and which was  
186 analyzed to provide an additional QC control for Nd. For the UMD1 solutions it was assumed  
187  $^{146}\text{Nd}/^{144}\text{Nd} = 0.7219$  and  $^{148}\text{Sm}/^{154}\text{Sm} = 0.49419$  as the internal correction values (13). Total  
188 intensity of the ion beams for samples and UMD1 deviated by no more than 15 % during the  
189 analysis with total Nd and Sm intensities of  $\sim 6.4$  V and 2.1 V, respectively, with all faraday cups  
190 having  $1 \times 10^{11} \Omega$  resistors.

191 A number of short-lived isobaric interferences for Nd and Sm exist in addition to  
192 naturally occurring isobars. The interferences for Nd include  $^{142}\text{Ce}$  and  $^{144,148,150}\text{Sm}$ , while Sm  
193 has interferences from  $^{144,148,150}\text{Nd}$  and  $^{151,152,154}\text{Eu}$ . Isobaric interferences for Nd were  
194 monitored during Nd analysis by using intensities of  $^{140}\text{Ce}$  and  $^{147}\text{Sm}$  as they do not have any  
195 isobaric interferences. The intensities of  $^{140}\text{Ce}$  and  $^{147}\text{Sm}$  and averaged approximately 3 mV and  
196 0.3 mV, respectively, while Sm interferences were monitored using  $^{145}\text{Nd}$  and  $^{153}\text{Eu}$  and were  
197 approximately 0.01 mV and 0.1 V respectively.

198

199 **Results**

200 Chemistry yields for Nd, Sm, and Gd were calculated by comparing the total ion  
201 intensities of the UMD1 samples to stock solutions of known concentration prepared  
202 gravimetrically prior to isotopic analysis. This resulted in yields of  $59 \pm 4\%$ ,  $53 \pm 10\%$ , and  $43 \pm$   
203  $6\%$  ( $2\sigma$ ) for Nd, Sm, and Gd respectively. Yields from BHVO-2 samples fall within these  
204 ranges with the noticeable exception of a calculated 80% yield for Gd. Concentrations for Nd  
205 and Sm in the MTR fuel solutions and their respective chemistry blank solutions contained in the  
206 Shielded Cells Facility at SRNL are presented in Table 3. Analysis of Gd in the MTR solutions  
207 showed no detectable signal.

208 The isotopic abundances of Nd and Sm in the MTR fuel and BHVO-2 were corrected  
209 using the mass fractionation correction terms derived from the UMD1 standards and the results  
210 are given in Table 4. The overall external reproducibility of the MC-ICP-MS is approximately  
211 0.02% ( $2\sigma$ ) and the bias introduced via the bracketing correction method is 0.01-0.4 %. Isobaric  
212 interferences from Nd on Sm were indistinguishable from measurement uncertainty. However,  
213 Sm interferences on Nd isotopic ratios required corrections on  $^{148}\text{Nd}$  and  $^{150}\text{Nd}$ . To perform this  
214 correction, the  $^{148}\text{Sm}/^{147}\text{Sm}$  and  $^{150}\text{Sm}/^{147}\text{Sm}$  ratios from the respective fuel assemblies were used  
215 in conjunction with the measured  $^{147}\text{Sm}$  monitored during Nd measurement to correct for  $^{148}\text{Sm}$   
216 and  $^{150}\text{Sm}$  on  $^{148}\text{Nd}$  and  $^{150}\text{Nd}$  for all of the fuel assemblies. The final abundances for Nd and Sm  
217 isotopes with the overall reproducibility, the bracketing bias, and isobaric interferences  
218 incorporated into the uncertainties are presented in Table 5.

219

220 **Discussion**

221 Yields and Blanks

222 Chemistry blank values for the fuel rod samples are far higher than those of the chemistry  
223 blank from UMD as expected from the hot cell work. The fuel rod blanks range from 2 µg to 1  
224 ng while the UMD blanks were between 2-3 pg. This difference in magnitude confirms that the  
225 separation process at UMD did not introduce a notable amount of natural lanthanoids which  
226 could have affected the isotopic signature of the fuel assemblies. Isotopic measurements of  
227 Blank A and Blank C show isotopic composition identical to their corresponding fuel samples,  
228 making it unlikely that the blanks were contaminated by legacy Savannah River Site processes  
229 that had been previously sampled in the Shielded Cells facility. The isotopic composition of  
230 Blank B was not measureable due to insufficient signal intensity for faraday cup measurements.  
231 Ion counters were not logistically practical due to concerns over residual radioactive  
232 contamination after the analyses and were not used for radioactive sample measurements. The  
233 UMD Blank, however, was measured using the ion counters and they were calculated assuming a  
234 natural isotopic composition. The similarity between the fuel rod isotopic composition and their  
235 respective blanks discredits the possibility of contamination from natural sources and instead  
236 implies that the blanks have been cross contaminated with the fuel rod material. Blank A has the  
237 highest amount of Nd and Sm while Blank B and C are approximately 10-1000 times lower. It is  
238 unclear where and how the contamination events occurred, but the contamination had no notable  
239 effect on the final reported isotopic compositions of the fuel assemblies.

240 Based on fission yields of Gd compared to Nd and Sm, Gd should have been produced in  
241 the sample however, no detectable signal was observed for Gd. Neutron induced fission of <sup>235</sup>U  
242 produces around 0.05% Gd and 3% Sm (3). The concentration of Sm in the MTR samples at  
243 UMD was on the order of micrograms. Therefore, Gd should have been present in the sample at

244 the ng level, well above the pg limit of detection when taking into account the 43% recovery.  
245 Therefore, the most probable reason for the lack of a Gd signal is a loss of the Gd cut from the  
246 2<sup>nd</sup> stage column. Unfortunately, operational restrictions on re-sampling the 50 mL solutions at  
247 SRNL resulted in an inability to reevaluate the procedure and determine the isotopic composition  
248 of Gd.

249 Another possible explanation for this low yield is that the Gd peak was eluted before or  
250 after the collection step. The Gd cut elutes over 4 mL of 0.15 M  $\alpha$ -HIBA so the possibility that  
251 the entire Gd peak was not collected is unlikely, especially when compared with the successful  
252 collection of Gd from the BHVO-2 samples.

253

#### 254 *Nd and Sm Isotope Abundances*

255 To determine if the burn-up of <sup>235</sup>U has any effect on the isotopic composition of the fuel  
256 assemblies, the ratio of fuel assemblies A:B and C:B are presented in Figures 2 and 3 with no  
257 decay corrections. In the case of Nd (Fig. 2) the final <sup>235</sup>U enrichment seems to have no effect  
258 on the production of Nd isotopes, with the exception of <sup>142</sup>Nd, <sup>143</sup>Nd, and <sup>144</sup>Nd. All of the listed  
259 exceptions could be explained due to differences in neutron fluence during reactor operation as  
260 reactions <sup>141</sup>Pr(n, $\beta$ )<sup>142</sup>Nd and <sup>143</sup>Nd(n, $\gamma$ )<sup>144</sup>Nd have thermal neutron capture cross sections of 11  
261 and 325 barns, respectively (14). While the <sup>141</sup>Pr capture cross section is small, the fission  
262 production of <sup>141</sup>Pr is relatively high at ~5.9% (3), which results in a large amount of available  
263 <sup>141</sup>Pr for neutron capture reactions to produce <sup>142</sup>Nd. The thermal capture cross section for  
264 <sup>142</sup>Nd(n, $\gamma$ )<sup>143</sup>Nd is similar to <sup>141</sup>Pr(n, $\beta$ )<sup>142</sup>Nd at 18 barns (14), however, due to the much lower  
265 total amount of available <sup>142</sup>Nd produced through neutron capture of <sup>141</sup>Pr and from fission ( $10^{-9}$

266 %) results in a negligible amount of  $^{142}\text{Nd}$  being converted to  $^{143}\text{Nd}$ . Therefore, higher neutron  
267 fluence has the overall effect of increasing the abundance of  $^{142,144}\text{Nd}$  in the nuclear fuel while  
268 decreasing the abundance of  $^{143}\text{Nd}$ .

269 The other isotopes of Nd (mass 145 through 150) do not show any obvious differences  
270 between the fuel assemblies. This is expected due to the low thermal neutron capture cross  
271 sections (50, 1.5, 2.6, and 1.0 barns for  $^{145}\text{Nd}$ ,  $^{146}\text{Nd}$ ,  $^{148}\text{Nd}$ , and  $^{150}\text{Nd}$ , respectively (14)) for  
272 these isotopes. Additionally, based on the reported burnup history of these fuels, it appears that  
273 the initial and final  $^{235}\text{U}$  enrichments of the fuel have no notable influence on  $^{145,146,148,150}\text{Nd}$   
274 abundances.

275 The graph of fuel rod A:B and C:B for Sm (Figure 3) notably shows more isotopic  
276 variation between the fuel samples for Sm as compared to Nd. The cause of the fluctuations for  
277  $^{147}\text{Sm}$ ,  $^{148}\text{Sm}$ ,  $^{149}\text{Sm}$ ,  $^{150}\text{Sm}$ , and  $^{151}\text{Sm}$  is likely due to thermal neutron captures on  $^{147}\text{Sm}$ ,  $^{149}\text{Sm}$ ,  
278 and  $^{151}\text{Sm}$  which have thermal capture cross sections of 57, 40,000, and 15,000 barns,  
279 respectively (14). Further evidence for neutron capture reactions causing the Sm isotopic  
280 differences between the fuel rods is seen in the enrichments in A:B mirrored by depletions in  
281 C:B and vice versa.

282 Interestingly,  $^{144}\text{Sm}$  is unique in that both fuel assemblies A and C are depleted relative to  
283 fuel rod B. As this isotope is not produced directly via  $^{235}\text{U}$  fission or neutron capture reactions,  
284 the  $^{144}\text{Sm}$  present is a remnant of natural Sm in either the nuclear fuel or the cladding material  
285 mixing with fission produced Sm which contains no  $^{144}\text{Sm}$ . To determine if the  $^{144}\text{Sm}$  is actually  
286 a sign of contamination from natural sources on the analyzed aliquots a simple calculation was  
287 used to determine the amount of natural Sm necessary to create the same isotopic composition in  
288 the fuel assemblies assuming an initial starting point of no Sm present. The resulting blank

289 contribution would need to be between 5 and 1500 times greater in the fuel samples than what  
290 was measured in the respective fuel blank samples. With the assumption of the  $^{144}\text{Sm}$  originating  
291 solely from natural Sm, there is approximately 4(1), 5(2), and 0.7(2)  $\mu\text{g}$  natural Sm in fuel  
292 assemblies A, B, and C, respectively. These masses result in Sm concentrations of 3(1), 3(2),  
293 and 0.6(2) ppm in the aluminum cladding which are less than the 5 ppm the American Society  
294 for Testing and Materials (ASTM) sets for high purity Al cladding (15). If the natural Sm came  
295 from the nuclear fuel instead of the cladding the concentrations would range between 11(3),  
296 35(11), and 2.6(9) ppm, well above the <3 ppm total lanthanoids the ASTM sets for enriched  
297 uranium (16). While assembly C is close to the limit, the 2.6(9) ppm value is for Sm only and it  
298 is reasonable to assume that the other lanthanoids would be present in similar quantities which  
299 would make the assembly not meet ASTM standards, therefore unlikely that the natural material  
300 came from the fuel itself.

301

## 302 **5.5 Conclusions**

303 A two stage separation technique involving cation exchange chromatography has successfully  
304 separated Nd and Sm from three MTR spent nuclear fuels. The isotopic abundances of Nd and  
305 Sm are distinctively non-natural and show depletions and enrichments in isotope pairs that have  
306 large cross sections for thermal neutron absorption and corresponding product nuclei with low  
307 thermal neutron absorption cross section. Signs of residual natural  $^{144}\text{Sm}$  originating from the  
308 cladding of the fuel samples are observed when comparing the Sm isotopic composition between  
309 the three fuel assemblies. The isotopic composition of Nd, with the exception of  $^{142}\text{Nd}$ ,  $^{143}\text{Nd}$ ,  
310 and  $^{144}\text{Nd}$ , is indistinguishable between the three nuclear fuel assemblies and is identical to  
311 predicted abundances derived from  $^{235}\text{U}$  fission. Sm isotopic compositions are more varied

312 between the fuels, which is attributed to differences in reactor neutron fluences and natural Sm  
313 contamination in the fuel cladding. Overall, the ability to isolate and analyze Nd and Sm from  
314 spent nuclear fuel using readily available materials and identified differences between three  
315 MTR spent nuclear fuels has been demonstrated.

316

- 317 1. IAEA (2010) Research reactors: purpose and future. (IAEA), p 15.
- 318 2. Weaver J, Biegalski SRF, & Buchholz BA (2009) Assessment of non-traditional isotopic  
319 ratios by mass spectrometry for analysis of nuclear activities. *Journal of Radioanalytical*  
320 *and Nuclear Chemistry* 282(3):709-713.
- 321 3. Chadwick MB, *et al.* (2011) ENDF/B-VII.1 Nuclear Data for Science and Technology:  
322 Cross Sections, Covariances, Fission Product Yields and Decay Data. *Nuclear Data*  
323 *Sheets* 112(12):2887-2996.
- 324 4. Bourgeois M, *et al.* (2011) Sm isotope composition and Sm/Eu ratio determination in an  
325 irradiated Eu-153 sample by ion exchange chromatography-quadrupole inductively  
326 coupled plasma mass spectrometry combined with double spike isotope dilution  
327 technique. *Journal of Analytical Atomic Spectrometry* 26(8):1660-1666.
- 328 5. Brennetot R, *et al.* (2005) Optimisation of the operating conditions of a MC-ICP-MS for  
329 the isotopic analysis of gadolinium in spent nuclear fuel using experimental designs.  
330 *Journal of Analytical Atomic Spectrometry* 20(6):500-507.
- 331 6. Isnard H, Brennetot R, Caussignac C, Caussignac N, & Chartier F (2005) Investigations  
332 for determination of Gd and Sm isotopic compositions in spent nuclear fuels samples by  
333 MC ICPMS. *International Journal of Mass Spectrometry* 246(1):66-73.
- 334 7. Kim JS, Jeon YS, Dal Park S, Han SH, & Kim JG (2007) Burnup determination of high  
335 burnup and dry processed fuels based on isotope dilution mass spectrometric  
336 measurements. *Journal of Nuclear Science and Technology* 44(7):1015-1023.
- 337 8. Kim JS, Jeon YS, Park YS, Park YJ, & Song K (2013) Simultaneous Determination of  
338 Caesium, Neodymium, Uranium and Plutonium Isotopes in Pressurized Water Reactor  
339 Spent Nuclear Fuels by Isotope Dilution Mass Spectrometry. *Asian Journal of Chemistry*  
340 25(12):7031-7033.
- 341 9. Gordon JR, Wong JW, MacMurray JS, Meissner SA, Scott RK, Conley C, Shipes R,  
342 SRNL-L4500-2013-00066; Savannah River National Laboratory: 2013.
- 343 10. Sharp N, McDonough WF, Ticknor, BW, Ash RD, Piccoli PM, & Borg DT (2014) Rapid  
344 analysis of trinitite with nuclear forensic applications for post-detonation material  
345 analyses. *Journal of Radioanalytical and Nuclear Chemistry* 302(1):57-67.
- 346 11. Hidaka H & Masuda A (1988) Nuclide analysis of rare earth elements of the Oklo  
347 uranium ore samples: a new method to estimate the neutron fluence. *Earth and Planetary*  
348 *Science Letters* 88(36):6.
- 349 12. Choppin GR & Silva RJ (1956) Separation of the lanthanides by ion exchange with  
350 alpha-hydroxy isobutyric acid. *Journal of Inorganic and Nuclear Chemistry* 3(2):153-  
351 154.
- 352 13. Wasserburg GJ, Jacobsen SB, Depaolo DJ, McCulloch MT, & Wen T (1981) Precise  
353 determination of Sm/Nd ratios, Sm and Nd isotopic abundances in standard solutions.  
354 *Geochimica Et Cosmochimica Acta* 45(12):2311-2323.
- 355 14. NNDC (National Nuclear Data Center, information extracted from the Chart of Nuclides  
356 database, <http://www.nndc.bnl.gov/chart/>).
- 357 15. ASTM Standard B209-14, 2014, "Aluminum and Aluminum Alloy-Sheet and Plate,"  
358 ASTM International, West Conshohocken, PA, 2014, DOI: 10.1520/B0209-14,  
359 [www.astm.org](http://www.astm.org).



360 16. ASTM Standard B209-14, 2013, "Uranium Metal Enriched to MOre than 15% and Less  
361 Than 20%," ASTM International, West Conshohocken, PA, 2013, DOI: 10.1520/C1462-  
362 00R13, [www.astm.org](http://www.astm.org).

363

**Table 1: Uranium enrichments of the three spent MTR nuclear fuels.**

	Initial $^{235}\text{U}$	Final $^{235}\text{U}$
A	93%	70%
B	93%	75%
C	45%	33%

**Table 2: Instrument operational conditions used for MC-ICP-MS analysis of MTR samples.**

**Nu Plasma HR MC-ICP-MS parameters**

RF Power	1300 W
Reflected Power	5 W
Accelerating Voltage	4000 V
Cool Gas Flow	13 L min <sup>-1</sup> Ar
Auxiliary Gas Flow	1 L min <sup>-1</sup> Ar
Sweep Gas Flow <sup>a</sup>	2.75 L min <sup>-1</sup> Ar
N <sub>2</sub> Gas	10 mL min <sup>-1</sup> N <sub>2</sub>
Aspiration Rate	50 μL min <sup>-1</sup>

Collector <sup>b</sup>	H5	H4	H3	H2	H1	Ax	L1	L2	IC0	L3
Nd	150	148	147	146	145	144	143	142		140
Sm <sup>c</sup>	154 5	152 3	151 2	150 1	149 50	148 9	147 8	146 7		144 5

<sup>a</sup>Gas flows are set with an Aridus I

<sup>b</sup>H/Lx cups refer to Faraday cups, IC0 is an ion counter

<sup>c</sup>Sm analyses involved two cycles: Cycle 1 | Cycle 2

**Table 3: Concentration of Nd and Sm ( $\mu\text{g}/\text{mL}$ ) in stock solutions at SRNL and total chemistry blank obtained at UMD. Blanks with no uncertainties correspond to blanks below limit of detection.**

	Nd	Sm
Fuel A	$1.3(3) \times 10^2$	14(4)
Blank A	$3.8(9) \times 10^{-2}$	$1.3(4) \times 10^{-2}$
Fuel B	$6(1) \times 10^2$	13(4)
Blank B	$1 \times 10^{-4}$	$2 \times 10^{-5}$
Fuel C	$3.1(7) \times 10^2$	6(2)
Blank C	$1.2(3) \times 10^{-2}$	$4 \times 10^{-5}$
UMD Blank	2 pg	3 pg

**Table 4: Nd and Sm isotopic ratios in MTR samples and natural materials with 2 $\sigma$  uncertainties.**

Sample (Nd)	$^{142}\text{Nd}/^{144}\text{Nd}$	$^{143}\text{Nd}/^{144}\text{Nd}$	$^{145}\text{Nd}/^{144}\text{Nd}$	$^{146}\text{Nd}/^{144}\text{Nd}$	$^{148}\text{Nd}/^{144}\text{Nd}$	$^{150}\text{Nd}/^{144}\text{Nd}$	Nd Beam (V)	$^{147}\text{Sm}$ (V)	$^{140}\text{Ce}$ (V)
A	0.00955(1)	0.61910(5)	0.50918(4)	0.46731(6)	0.24410(6)	0.08862(3)	5.39	0.00303	0.00026
B	0.00724(1)	0.70851(9)	0.55239(2)	0.47651(7)	0.25761(7)	0.09564(3)	4.80	0.00023	0.00036
C	0.00215(1)	0.93197(9)	0.63756(4)	0.52532(7)	0.29817(8)	0.10887(4)	5.42	0.00147	0.00008
BHVO-2 1	1.14038(6)	0.51264(2)	0.34861(1)	0.72278(4)	0.24213(3)	0.23718(3)	6.29	0.00258	0.01340
BHVO-2 2	1.14193(5)	0.51301(2)	0.34839(1)	0.72180(3)	0.24147(2)	0.23621(2)	7.18	0.00003	0.00142
Ames (n=2)	1.14173(5)	0.51213(2)	0.34840(1)	0.72190 <sup>a</sup>	0.24154(1)	0.23630(2)	6.69	0.00000	0.00009
UMD1 (n=3)	1.14173(40)	0.51239(11)	0.34839(5)	0.72190 <sup>a</sup>	0.24156(3)	0.23630(6)	7.03	0.00002	0.00125

Sample (Sm)	$^{151}\text{Sm}/^{154}\text{Sm}$	$^{144}\text{Sm}/^{154}\text{Sm}$	$^{147}\text{Sm}/^{154}\text{Sm}$	$^{148}\text{Sm}/^{154}\text{Sm}$	$^{149}\text{Sm}/^{154}\text{Sm}$	$^{150}\text{Sm}/^{154}\text{Sm}$	$^{152}\text{Sm}/^{154}\text{Sm}$	Sm Beam (V)	$^{146}\text{Nd}$ (V)	$^{153}\text{Eu}$ (V)
A	0.1676(2)	0.00206(10)	11.7550(5)	3.5148(7)	0.1732(2)	8.9301(36)	4.5568(6)	2.21	0.00007	0.7
B	0.3687(3)	0.00475(14)	21.185(16)	3.4269(11)	0.4646(2)	12.7430(69)	7.8544(13)	2.28	0.00010	0.1
C	0.6589(5)	0.00134(14)	22.336(14)	1.5066(3)	0.6811(2)	11.8466(44)	7.9488(7)	2.19	0.00002	0.2
BHVO-2 1	n/a <sup>c</sup>	0.13537(4)	0.6599(1)	0.49466(4)	0.60811(8)	0.32472(4)	1.17586(3)	2.16	0.0008	0.02
BHVO-2 2	n/a <sup>c</sup>	0.13538(4)	0.65984(9)	0.49452(3)	0.60799(6)	0.32465(4)	1.17574(3)	2.18	0.0001	0.03
UMD1 (n=4)	n/a <sup>c</sup>	0.13527(4)	0.65937(6)	0.49419 <sup>b</sup>	0.60769(3)	0.32450(6)	1.17549(3)	2.01	0.00001	0.0003

<sup>a</sup> $^{146}\text{Nd}/^{144}\text{Nd} = 0.7219$  for mass fractionation correction

<sup>b</sup> $^{148}\text{Sm}/^{154}\text{Sm} = 0.49419$  for mass fractionation correction

<sup>c</sup>No  $^{151}\text{Sm}$  exists in natural samples

**Table 5: Isotope abundances of Nd and Sm in the three MTR fuels.**

Nd Isotope	A	B	C
<sup>142</sup> Nd	0.3250(3)%	0.2336(2)%	0.0615(2)%
<sup>143</sup> Nd	21.073(5)%	22.871(6)%	26.597(6)%
<sup>144</sup> Nd	34.038(1)%	32.280(1)%	28.539(1)%
<sup>145</sup> Nd	17.332(2)%	17.831(2)%	18.195(2)%
<sup>146</sup> Nd	15.907(2)%	15.382(2)%	14.992(2)%
<sup>148</sup> Nd	8.309(2)%	8.316(3)%	8.509(3)%
<sup>150</sup> Nd	3.016(1)%	3.087(1)%	3.107(1)%
Sm Isotope	MTR 2009	MTR 2010	MTR 2011
<sup>147</sup> Sm	39.06(2)%	45.03(4)%	48.58(6)%
<sup>148</sup> Sm	11.678(4)%	7.284(3)%	3.277(1)%
<sup>149</sup> Sm	0.576(1)%	0.988(1)%	1.481(1)%
<sup>150</sup> Sm	29.67(1)%	27.09(2)%	25.77(1)%
<sup>151</sup> Sm	0.557(1)%	0.784(1)%	1.433(1)%
<sup>152</sup> Sm	15.140(4)%	16.695(7)%	17.288(6)%
<sup>154</sup> Sm	3.3225(3)%	2.126(1)%	2.175(1)%

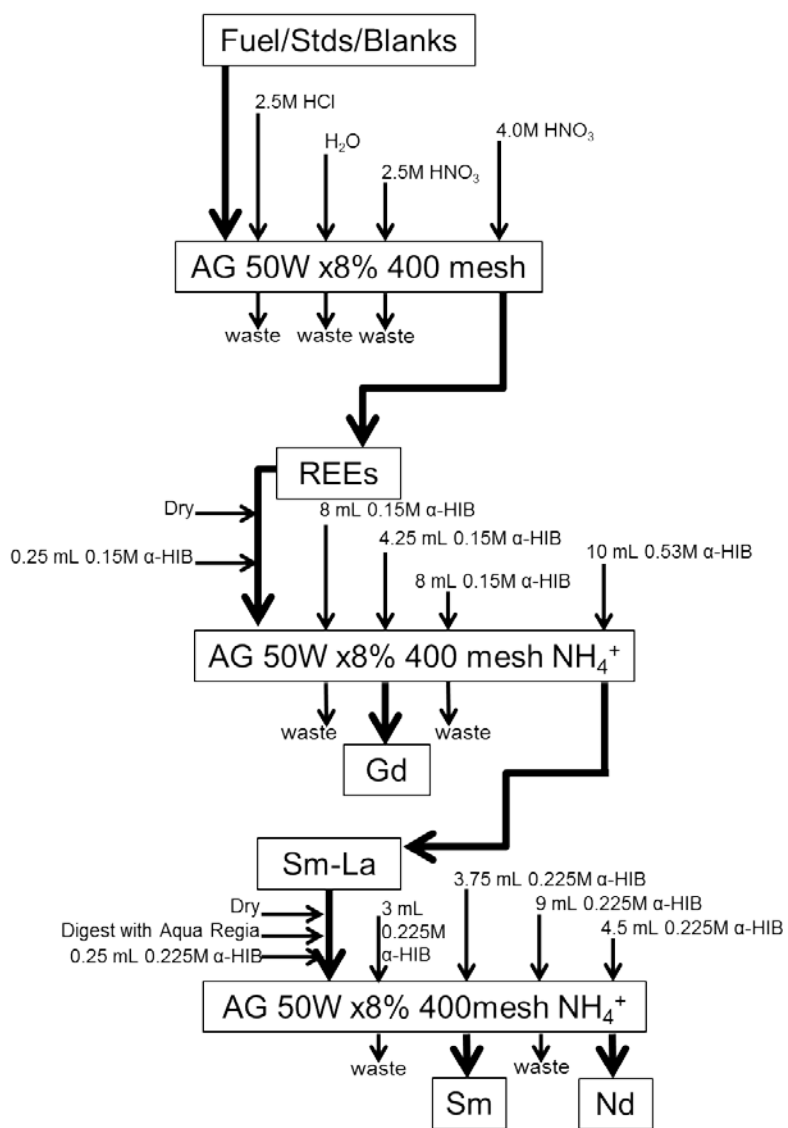
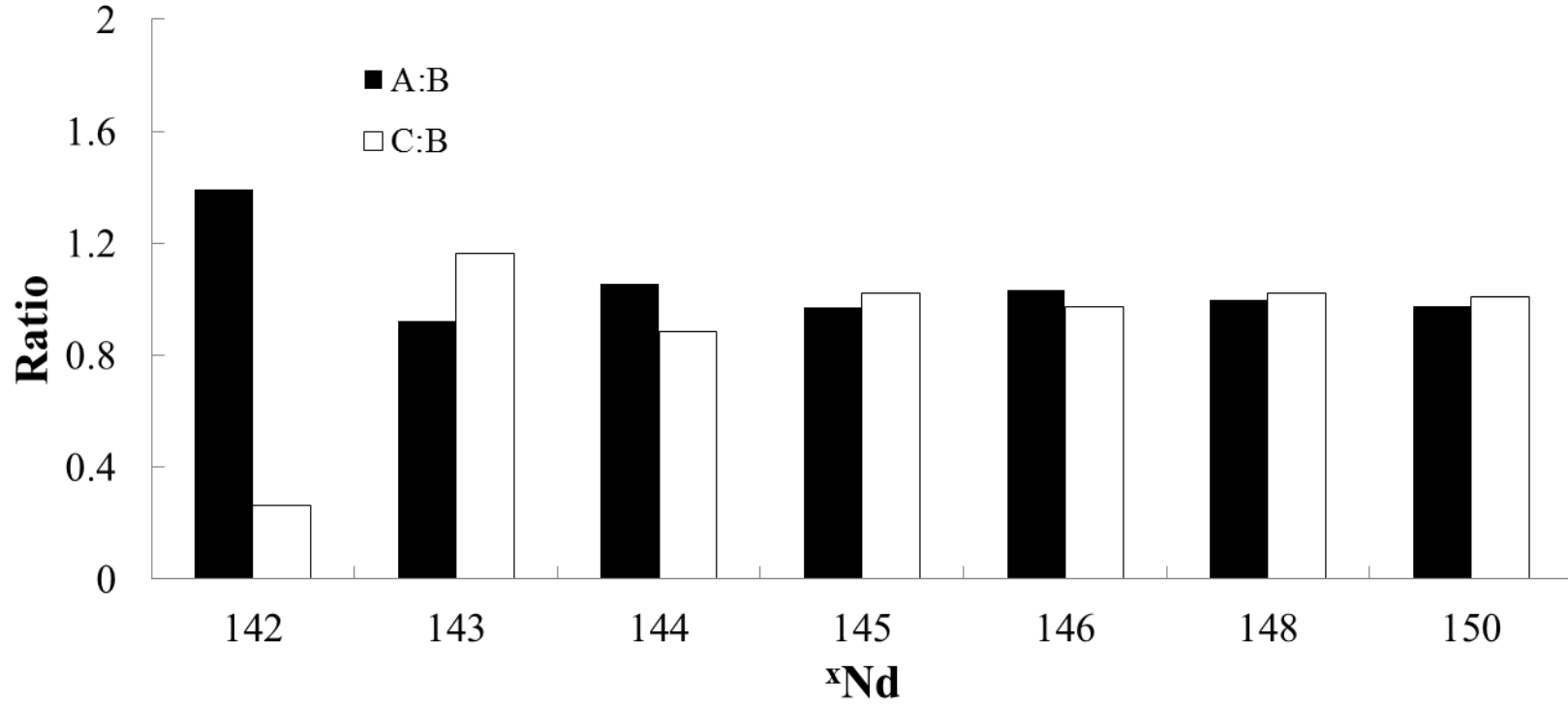
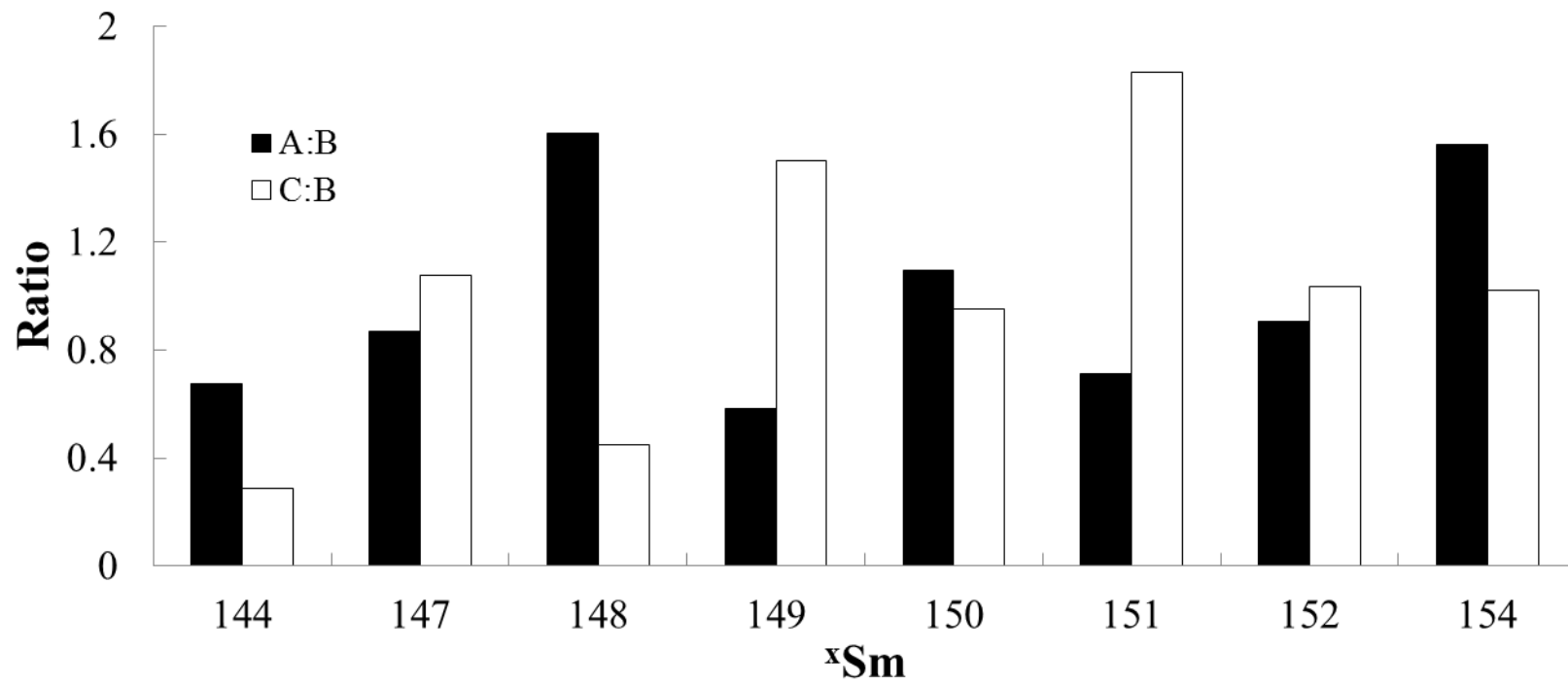


Figure 1: Separation schematic for isolating Gd, Sm, and Nd. Bold lines denote analyte path.



**Figure 2: Ratio of Nd isotope abundance of fuel rods A and C to B. Uncertainty is indistinguishable at the above scale.**





**Figure 3: Ratio of Sm isotope abundance of fuel rods A and C to B. Uncertainty is indistinguishable at the above scale.**